

COUPLING MATRIX FOR BOUNDARY CELLS OF A CARTESIAN GRID METHOD USING A TRANSFER-MATRIX METHOD

7TH EUROPEAN CONFERENCE ON COMPUTATIONAL FLUID
DYNAMICS (ECFD 7)

(ECCM –ECFD 2018 CONFERENCE)

JUNYA IMAMURA¹

¹*imi* Computational Engineering Laboratory
Wako-shi, Honcho 31-9-803, Saitama/Japan, 351-0114
jimamura@ra2.so-net.ne.jp

Key words: Coupling matrix, Transfer-matrix method, Reduction method, Boundary cell, Cartesian grid method, C^1 -continuity element, Immersed boundary method.

Abstract. The objective of the immersed boundary method that was spotlighted in recent years is to immerse a coupling matrix into the boundary cells of a Cartesian grid method.

The transfer-matrix method (also referred to as the reduction method) automatically includes a coupling matrix by providing a rigid element and can easily partially include very large stiffness elements. It means that the method proposed in this paper can be applied not only for boundary cells but is also applicable for general surface cells.

In this study, a transfer matrix is used to induce stiffness matrix for boundary and surface cells to solve continuum-mechanics problems using a displacement method.

C^0 -continuity boundary cells for flow fields are used to explain the scheme. Then, C^1 -continuity elements used for solving the plate-bending problem are explained. As a benchmark test, a circular plate is viewed, which logically must include a coupling matrix in this case by the Cartesian grid method, and is a known exact solution for the problem.

1 INTRODUCTION

The objective of the immersed boundary method spotlighted in recent years is to immerse a coupling matrix into the boundary cells of a Cartesian grid method.

The transfer-matrix method (reduction method) automatically includes a coupling matrix by providing a rigid element. This method can easily include portions of extremely large stiffness elements. This means that the method proposed herein can be applied for surface cells in general and to the normal boundary cells.

The transfer-matrix method can be applied to one-dimensional problems [1]. However, methods that are reliable for two- and three-dimensional problems are difficult to find.

Even for one-dimensional problems, the application of transfer-matrix method is difficult depending on the framework, and it is applied elegantly only for the continuous-beam case or the closed (tree-like) framework [2]. The method cannot be used for enclosed (network-like)

frameworks [3].

Therefore, the transfer matrix is helpful for generating a stiffness matrix (e.g. to introduce an arch into a framework) to use in a displacement method [4]. The application of the transfer matrix for this objective is flexible and tolerates the rigid parts in the beam mentioned above.

In this study, the transfer-matrix method is applied to generate stiffness matrices for the boundary and surface cells of a Cartesian grid in 2D and 3D.

C^0 -continuity boundary cells are introduced for flow fields to explain the scheme; then, C^1 -continuity elements for the plate-bending problem is described. A benchmark test using a circular plate will be discussed to explain the generality of the proposal.

A novel reduction method for continuum mechanics and a generalised force method was proposed previously [5] [6], to solve an impossible case for the displacement method.

Both methods simultaneously solve an equation that was constructed using both equilibrium and compatibility equations. For example, at nodes wherein the four-vertex nodes of the finite elements are joined, four displacement parameters of individual elements are used as the unknowns of the systems. Against those formulae are sets comprising one equilibrium and three compatible conditions $d_A = d_B = d_C$ simultaneously.

The primary technique uses an absolute-maximum pivot element to eliminate one parameter for the Gaussian method using a sweep-out step that includes swapping columns.

This method is an intrinsic displacement method; therefore, the elements require C^0 -continuity and are sufficient, but impossible by the displacement method only.

The C^1 -continuity elements are used to construct a coupling matrix for plate bending, for example, to transfer the state vector (displacements $\{w, \theta\}$ and forces $\{M, Q\}$).

The transfer matrix for a bending beam is obtained by starting with the equilibrium equation $D \cdot \partial^4 w / \partial x^4 + q = 0$, where D is stiffness of the beam, w is the deflection and q is the vertical load, calculated by repeated integration $\rightarrow Q_L + \dots = 0 \rightarrow M_L + \dots = 0 \rightarrow \theta_L + \dots = 0 \rightarrow w_L + \dots = 0$ as Eq. (1) in a homogeneous case, wherein the suffix L indicates the left side of the beam, Q is the shearing force, M is the momentum and θ is the inclination. Eq. (1) can be represented by Eq. (2) in a matrix form (without $\partial^4 w / \partial x^4$ row).

$$\left. \begin{aligned}
 w_L + (1+x)\theta_L + (1+x+\frac{x^2}{2})\frac{M_L}{D} + (1+\dots+\frac{x^3}{6})\frac{Q_L}{D} &= 0 \\
 \uparrow \\
 \theta_L + (1+x)\frac{M_L}{D} + (1+x+\frac{x^2}{2})\frac{Q_L}{D} + \frac{\partial w}{\partial x} &= 0 \\
 \uparrow \\
 M_L + (1+x)Q_L + D\frac{\partial^2 w}{\partial x^2} &= 0 \\
 \uparrow \\
 Q_L + D\frac{\partial^3 w}{\partial x^3} &= 0 \\
 \uparrow \\
 \frac{\partial^4 w}{\partial x^4} &= 0
 \end{aligned} \right\} \quad (1)$$

$$\mathbf{Z}_x \equiv \begin{Bmatrix} \mathbf{d} \\ \mathbf{K} \end{Bmatrix}_x = \begin{bmatrix} \mathbf{T} \end{bmatrix} \begin{Bmatrix} \mathbf{d} \\ \mathbf{K} \end{Bmatrix}_L \quad (2)$$

Let us refer to the vector $\mathbf{Z} \equiv \{\mathbf{d}, \mathbf{K}\}$ as the state vector, where \mathbf{d} is the displacement vector, \mathbf{K} is the force vector and $[\mathbf{T}]$ is the transfer matrix that transfers \mathbf{Z}_L to a point x from the left side of the beam.

Eq. (1) generates the transfer matrix bottom-up, but it can also be generated top-down if $[\mathbf{T}]$ is represented as a finite Taylor series, similar to that in Eq. (3).

Eq. (3), for a one-dimensional problem, can be easily developed for the two- or three-dimensional problems using top-down methods in a non-homogeneous case.

$$\begin{bmatrix} \mathbf{T} \end{bmatrix} = \begin{bmatrix} 1 & x & \frac{x^2}{2} & \frac{x^3}{6} & \frac{x^4}{24D} \\ & 1 & x & \frac{x^2}{2} & \frac{x^3}{6D} \\ & & \vdots & & \\ & & & & 1 \end{bmatrix} \cdot \begin{bmatrix} (\frac{d^j w}{dx^j})_i \end{bmatrix} = \begin{bmatrix} \frac{d^i}{dx^i} \left(\sum_{j=0}^{4-i} \frac{x^j}{j!} w^{(j)} + \frac{1}{D} \frac{x^{(5-i)}}{(5-i)!} w^{(5-i)} \right) \end{bmatrix} \quad (3)$$

2 COUPLING MATRICES FOR BOUNDARY CELLS BY TRANSFER MATRIX

2.1 Displacement vector u represented by finite Taylor series

The time-axially central difference methods are applied to obtain velocities and accelerations using the displacement vector u as variables. The velocity vector is represented in \mathbf{U} .

Let u_i be a three-fold third-order element. The Maclaurin expansion of u_i is represented in Eq. (4) using coordinates local to the origin of the gravity point of a finite element, where the T indicates transportation. The equivalent finite Taylor series can be represented similarly using $(\Delta x, \Delta y, \Delta z)$.

$$u_i = \{1, x, y, z, xy, yz, zx, xyz\} \{u_i^{(000)} u_i^{(100)} u_i^{(010)} u_i^{(001)} u_i^{(110)} u_i^{(011)} u_i^{(101)} u_i^{(111)}\}_0^T \quad (4)$$

2.2 State vector represented by transfer matrix

Let $u_i^{(lmn)}$ be the derivative of u_i . Eq. (5) is a transfer equation from the local origin to (x, y, z) point that uses a transfer matrix for the vector derivative $\{\mathbf{d}, \mathbf{L}\}$, distinguished from the state vector $\{\mathbf{d}, \mathbf{K}\}$. The components $L_i^{(lmn)}$ of the vector $\{\mathbf{L}\}$ are conserved variable parameters that multiply the viscous coefficient μ to $u_i^{(lmn)}$. The case $\mu = \infty$ indicates coupling.

$$\begin{aligned}
 \begin{Bmatrix} \mathbf{d} \\ \mathbf{L} \end{Bmatrix}_0 &\equiv \{u_i^{(000)} L_i^{(100)} L_i^{(010)} L_i^{(001)} L_i^{(110)} L_i^{(011)} L_i^{(101)} L_i^{(111)}\}_0 \\
 \begin{Bmatrix} u_i^{(000)} \\ L_i^{(100)} \\ L_i^{(010)} \\ L_i^{(001)} \\ L_i^{(110)} \\ L_i^{(011)} \\ L_i^{(101)} \\ L_i^{(111)} \end{Bmatrix}_{x,y,z} &= \begin{bmatrix} 1, (x, y, z) / \mu, (xy, yz, zx | xyz) / \mu^2 \\ 0 | 1, 0, 0 | (y, 0, z | yz) / \mu \\ 0 | 0, 1, 0 | (x, z, 0 | xz) / \mu \\ 0 | 0, 0, 1 | (0, y, x | xy) / \mu \\ 0 | 0, 0, 0 | 1, 0, 0 | z \\ 0 | 0, 0, 0 | 0, 1, 0 | y \\ 0 | 0, 0, 0 | 0, 0, 1 | x \\ 0 | 0, 0, 0 | 0, 0, 0 | 1 \end{bmatrix} \begin{Bmatrix} \mathbf{d} \\ \mathbf{L} \end{Bmatrix}_0^T
 \end{aligned} \tag{5}$$

The components of the stress vector $\{\mathbf{K}\}$ are represented as linear combinations of the components $L_i^{(lmn)}$. Let the state vector $\{\mathbf{Z}\} \equiv \{\mathbf{d}, \mathbf{K}\}^T$ be represented as in Eq. (6).

$$\{\mathbf{Z}\} = [\mathbf{T}]\{\mathbf{Z}\}_0 \equiv \begin{Bmatrix} \mathbf{d} \\ \mathbf{K} \end{Bmatrix} = \begin{bmatrix} \mathbf{T}_d \\ \mathbf{T}_K \end{bmatrix} \begin{Bmatrix} \mathbf{d} \\ \mathbf{K} \end{Bmatrix}_0 \tag{6}$$

The state vector in Eq. (7) is represented in detail using linear combinations.

$$\{\mathbf{Z}\} \equiv \begin{Bmatrix} \mathbf{d} \\ \mathbf{K} \end{Bmatrix} \equiv \begin{Bmatrix} u_1 \\ u_2 \\ u_3 \\ \sigma_{11} \\ \sigma_{22} \\ \sigma_{12} \\ \sigma_{33} \\ \sigma_{13} \\ \sigma_{23} \end{Bmatrix} = \begin{Bmatrix} u_1 \\ u_2 \\ u_3 \\ L_1^{(100)} \\ L_2^{(010)} \\ L_2^{(010)} + L_1^{(100)} \\ L_3^{(001)} \\ L_1^{(001)} + L_3^{(100)} \\ L_3^{(010)} + L_2^{(001)} \end{Bmatrix} \tag{7}$$

2.3 Mathematical domains in the cell and parameters

Let us consider a cell comprising two phases, A and B, and refer to these as domain A and domain B. The coupling matrix for the boundary can be obtained by assigning $\mu = \infty$ for domain B. The proposed method is applicable to general two-phase problems and can be extended to N-phases problems, such as a model of a liquid–air–solid system.

First, let us consider the mathematical domains for individual phases, which occupy the whole cell, and are represented using parameters $\{u_i\}_k$ at the vertex node k of each voxel individually.

Then, following the above discussion, let us set parameters $\{u_i^{(110)}\}_{C\langle x-y \rangle}$, $\{u_i^{(101)}\}_{C\langle x-z \rangle}$, $\{u_i^{(011)}\}_{C\langle y-z \rangle}$ at the centroid of the inter-element boundaries, where suffixes indicate, $C\langle x-y \rangle$ on the centroid of the $\langle x-y \rangle$ plane and they are constant parameters over the whole plane. These are used to offset the distortion of the element functions. These offsets measure the extent of numerical locking.

In addition, let us set a parameter $\{u_i^{(111)}\}_{\text{COG}}$ on the centre of the gravity to measure pseudo-body forces.

2.4 Immersion of the coupling matrix into Cartesian grid cells

The immersion of the coupling matrix into Cartesian grid cells is realised by eliminating the A-phase parameters located mathematically in the B-domain and vice versa. Specifically, this step eliminates a total of 24 overlap parameters at eight nodes.

Figure 1 shows all four possible patterns with one node, two nodes, three nodes, and four nodes in an area. This parameter is the number of connections between surface and element.

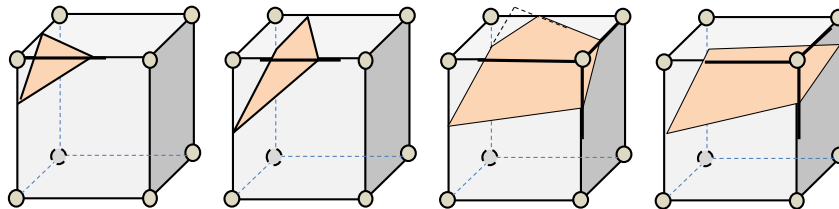


Figure 1: Patterns between the surface and domains A / B

The axes of the Cartesian grid penetrate at three, four and five crossing points. To eliminate the 24 parameters in descending order, 8 conditions, 6 conditions and $4 + 4/5$ (when simply apportioned) conditions per node are required.

The eliminated conditions are formularised in terms of local coordinates (s_1, s_2, n) on the surface, where n is the direction normal to the surface. Figure 2 shows the n -direction in the two-dimensional case.

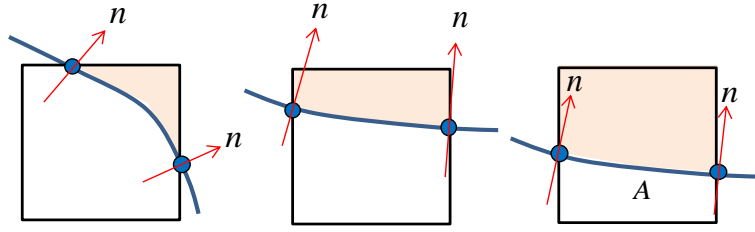


Figure 2: Normal direction of the local coordinates to formularise the eliminated conditions

For the case of four crossing points, 6 eliminated conditions are required, and these are sufficient. These eliminations equate the displacements $\{u_{s1}, u_{s2}, u_n\}$ and stresses $\{\sigma_n, \tau_{sn}, \omega_{sn}\}$ of the two domains at the four crossing points.

In the other two cases, however, the least-squares or similar method must be applied.

For the five-crossing-points case, the conditions for four crossing points case are used with the least-squares method.

For the three-crossing-points case, gradient components of the above cases, i.e. $\partial (u_{s1}, u_{s2}, u_n) / \partial s_i$ and $\partial (\sigma_n, \tau_{sn}, \omega_{sn}) / \partial s_i$ per node, must be added, or more one point must be added onto the centroid of the boundary surface to apply the same scheme to above four crossing.

The scheme for eliminating surplus parameters is shown in a plate bending case in the following chapter.

3 PLATE BENDING

3.1 Transfer matrix for plate bending

The equilibrium equation for the Kirchhoff plate-bending model is shown in Eq. (8), the transfer matrix for the vector derivative in Eq. (9), and the state vector in Eq. (10), where D is the plate-bending rigidity, w is the deflection and q is the distributed load.

$$D \cdot \nabla^2 \nabla^2 w = q \quad (8)$$

$$\begin{Bmatrix} w^{(00)} \\ w^{(10)} \\ w^{(01)} \\ Dw^{(20)} \\ Dw^{(11)} \\ \vdots \\ D^2 w^{(33)} \end{Bmatrix} = \begin{bmatrix} 1 & x & y & \frac{1}{2D} x^2 & \frac{xy}{D} & \dots & \frac{1}{36D^2} xy^3 \\ & 1 & \frac{x}{2D} & \dots & & & \\ & & 1 & \dots & & & \\ & & & 1 & \dots & & \\ & & & & 1 & 0 & \dots \end{bmatrix} \cdot \begin{Bmatrix} w^{(00)} \\ w^{(10)} \\ w^{(01)} \\ Dw^{(20)} \\ Dw^{(11)} \\ \vdots \\ D^2 w^{(33)} \end{Bmatrix}_0 \quad (9)$$

$$\begin{Bmatrix} \mathbf{d} \\ \mathbf{K} \end{Bmatrix} = \begin{bmatrix} & \\ \mathbf{T} & \end{bmatrix} \cdot \begin{Bmatrix} \mathbf{d} \\ \mathbf{K} \end{Bmatrix}_0, \text{ where } \{\mathbf{d}\} \equiv \begin{Bmatrix} w^{(00)} \\ w^{(10)} \\ w^{(01)} \end{Bmatrix} \quad (10)$$

3.2 Elimination scheme of the surplus parameters

Let us define the local origin for the two domains A and B individually on the diagonal points in Figure 3, then let (1) and (2) be the number of the tow crossing point in the forgoing Figure 2. ($\{\mathbf{K}\}_{A(0)}, \{\mathbf{K}\}_{B(0)} \leftarrow \{\mathbf{L}\}_{A(0)}, \{\mathbf{L}\}_{B(0)}$)

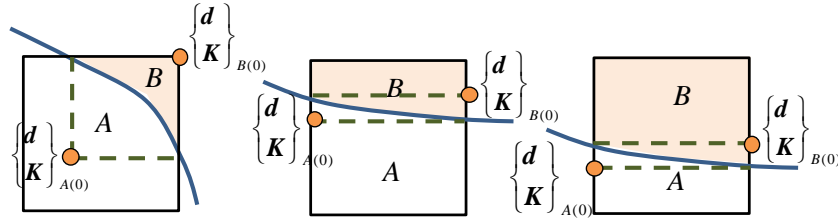


Figure 3: Definition of the individual local origin for two domains A and B

The state vectors on the crossing points in individual inside of the two domains shown in Figure 4 can be represented by transferring from the individual origin.

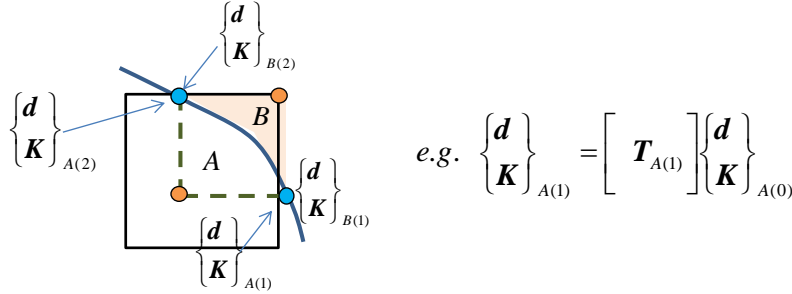


Figure 4: State vectors on crossing point in individual domain side

It is firstly shown in Eq. (11) how to equate above state vectors on the crossing points, then we obtain the objective coupling matrix $[C_{oupl}]$ showing in Eq. (12).

We can accomplish the purpose to obtain the function in boundary cells representing with the parameters on the vertex nodes $\{\mathbf{d}\}_1-\{\mathbf{d}\}_4$ shown in Figure 5 by Eq. (13) using $\{\mathbf{d}, \mathbf{K}\}_{B(0)}$ and $\{\mathbf{d}, \mathbf{K}\}_{A(0)}$ which is represented again with the former, and the former can be represented through a coupling matrix with $\{\mathbf{d}, \mathbf{K}\}_0$ which is the state vector on the centre of the gravity.

$$\left. \begin{aligned}
 & \left\{ w, \frac{\partial w}{\partial s}, \right. \\
 & \left. \theta_n, \frac{\partial \theta}{\partial s}, \right. \\
 & \left. M_n, \frac{\partial M_n}{\partial s}, \right. \\
 & \left. Q_n, \frac{\partial Q_n}{\partial s} \right\}_{(1)} \\
 & \equiv \left\{ \mathbf{Z}_{A(1)} \right\} = \left[\mathbf{F}_{A(1)} \right] \left\{ \begin{array}{l} \mathbf{d} \\ \mathbf{K} \end{array} \right\}_{A(0)} \\
 & \left\{ \mathbf{Z}_{A(1)} \right. \\
 & \left. \mathbf{Z}_{A(2)} \right\} = \left[\begin{array}{l} \mathbf{F}_{A(1)} \\ \mathbf{F}_{A(2)} \end{array} \right] \left\{ \begin{array}{l} \mathbf{d} \\ \mathbf{K} \end{array} \right\}_{A(0)} \\
 & \text{equate: } \left\{ \begin{array}{l} \mathbf{Z}_{A(1)} \\ \mathbf{Z}_{A(2)} \end{array} \right\}_{A(0)} = \left\{ \begin{array}{l} \mathbf{Z}_{A(1)} \\ \mathbf{Z}_{A(2)} \end{array} \right\}_{B(0)}
 \end{aligned} \right\} \quad (11)$$

$$\therefore \left\{ \begin{array}{l} \mathbf{d} \\ \mathbf{K} \end{array} \right\}_{A(0)} = \left[\begin{array}{l} \mathbf{F}_{A(1)} \\ \mathbf{F}_{A(2)} \end{array} \right]^{-1} \left[\begin{array}{l} \mathbf{F}_{B(1)} \\ \mathbf{F}_{B(2)} \end{array} \right] \left\{ \begin{array}{l} \mathbf{d} \\ \mathbf{K} \end{array} \right\}_{B(0)} \Rightarrow \left\{ \begin{array}{l} \mathbf{d} \\ \mathbf{K} \end{array} \right\}_{A(0)} = \left[\mathbf{C}_{oupl} \right] \left\{ \begin{array}{l} \mathbf{d} \\ \mathbf{K} \end{array} \right\}_{B(0)} \quad (12)$$

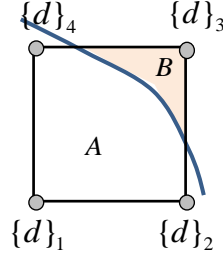


Figure 5: Numbering for the vertex nodes using in Eq. (13), in where for an example

$$\left\{ \begin{array}{l} \mathbf{d}_1 \\ \mathbf{d}_2 \\ \mathbf{d}_3 \\ \mathbf{d}_4 \end{array} \right\} = \left[\begin{array}{l} \left[\begin{array}{l} T_{1dA} \\ T_{2dA} \end{array} \right] \\ \left[\begin{array}{l} T_{3dB} \\ T_{4dB} \end{array} \right] \end{array} \right] \mathbf{C}_{oupl} \left\{ \begin{array}{l} \mathbf{d} \\ \mathbf{K} \end{array} \right\}_{B(0)} \quad \therefore \left\{ \begin{array}{l} \mathbf{d} \\ \mathbf{K} \end{array} \right\}_{B(0)} = \left[\begin{array}{l} \left[\begin{array}{l} T_{1dA} \\ T_{2dA} \end{array} \right] \\ \left[\begin{array}{l} T_{3dB} \\ T_{4dA} \end{array} \right] \end{array} \right] \mathbf{C}_{oupl} \left\{ \begin{array}{l} \mathbf{d}_1 \\ \mathbf{d}_2 \\ \mathbf{d}_3 \\ \mathbf{d}_4 \end{array} \right\} \quad (13)$$

3.3 Benchmark test problem

A circular plate with a fixed boundary bent under a uniform load is chosen for benchmark testing. The exact solution is known: $w_{exact} = 1/64 (10^3 qr^4/D) = 15.625 (qr^4/D)$.

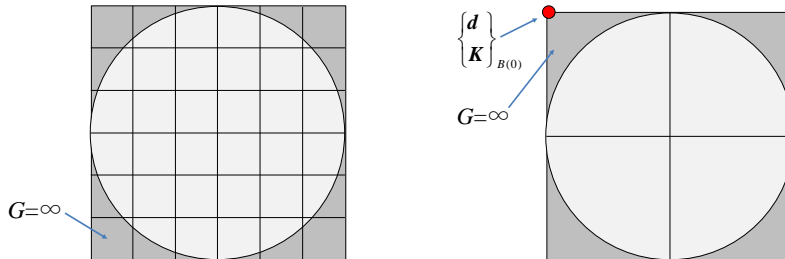


Figure 3: Benchmark test problem (circular plate bending)

We can easily and logically recognize that the objective is achieved to immerse the coupling matrix into boundary cells, with the righthand side Figure. The numerical scheme and accuracy of the solution using C^1 -continuity element for Kirchhoff theory is another theme [7].

4 CONCLUSIONS

- The proposed transfer-matrix method immerses a coupling matrix into boundary cells, and immerses a stiffness matrix into surface cells for using in the Cartesian grid method.
- The proposed method is verified in calculations solving the circular plate-bending problem with a fixed end boundary around the plate under a uniform load, for which the exact solution is known.

REFERENCES

- [1] S. Falk, Berechnung des beliebig gestützten Durchlaufträgers nach dem Reduktionsverfahren, *Ingenieur-Archiv*, (1956)24:216-232.
- [2] S. Falk, Die Berechnung offener Rahmentragwerkennach dem Reduktionsverfahren, *Ingenieur-Archiv*, (1958)26:61-80.
- [3] S. Falk, Die Berechnung geschlossener Rahmentragwerken nach dem Reduktionsverfahren, *Ingenieur-Archiv*, (1958)26:96-109.
- [4] E. Knopf, Elektronische Berechnung von Stabtragwerken, *Konstruktiver Ingenieurbau, Berichte Heft 3*, Institut für Konstruktiven Ingenieurbau der Ruhr-Universität Bochum, Vol.3, Vulkan-Verlag, 1969.
- [5] J. Imamura and T. Tanahashi, An application of the reduction method to continuum mechanics, *Proceedings of applied mechanics*, JSCE, Vol.2, pp.241-252, 1999.
- [6] J. Imamura, Generalized force method (GFM) and a numerical solution of the simultaneous equation, *Proceedings of applied mechanics*, JSCE, Vol.19, J-STAGE, 2016.
- [7] J. Imamura, Study on C^1 -continuity elements and application to Kirchhoff plate bending, and introduction of transverse shear deformation, *Proceedings of the conference on computational engineering and science*, JSCES, Vol.22, 2017.